

# Detection of Different Tissue Types of Colorectal Cancer Based on Histological Images Using Deep Learning Approach

## Derin Öğrenme Yaklaşımı Kullanılarak Histolojik Görüntülere Dayalı Kolorektal Kanserin Farklı Doku Tiplerinin Saptanması

Emek GÜLDOĞAN<sup>a</sup>, Zeynep KÜÇÜKAKÇALI<sup>a</sup>, Hasan UCUZAL<sup>a</sup>, Cemil ÇOLAK<sup>a</sup>

<sup>a</sup>Department of Biostatistics and Medical Informatics, İnönü University Faculty of Medicine, Malatya, TURKEY

**ABSTRACT Objective:** Automatic machine learning methods developed by employing deep learning approaches have been the focus of numerous studies nowadays. The objective of the current study is to design a web-based software that is used in the classification of tissue samples in colorectal cancer, based on eight different histopathological tissue types, to support physicians for the clinical diagnosis of colorectal cancer, and thus to enable physicians to make quick and accurate decisions. **Material and Methods:** An open-access data set (DOI: 10.5281/zenodo.53169) consisting of 5,000 histopathological images, including different histopathological tissue types of colorectal cancer, was used in the present study. Keras-based AutoKeras library was applied to classify the histopathological tissue types of colorectal cancer. Appropriate python language libraries were employed in the development of the web-based software. A deep learning-based model was constructed to predict eight histopathological tissue types of colorectal cancer. **Results:** The highest metric values among the performance criteria achieved for different tissue types of colorectal cancer were calculated for adipose type, and we found that accuracy was 0.996, sensitivity 0.992, specificity 0.996, precision 0.974, recall 0.992, and F<sub>1</sub>-score 0.983, respectively. This research differs from other studies in that it includes open access software. **Conclusion:** The web software based on the model proposed in this study provided promising predictions in classifying different tissue types from histopathological images of colorectal cancer. Thanks to the proposed software, the tissue types of colorectal cancer are easily understood by medical professionals and other healthcare workers. Hence, the workload of medical professionals can be reduced, and a faster consultation system can be formed.

**Keywords:** Multiple classification; tissue types; colorectal cancer; deep learning architecture; Keras/AutoKeras

**ÖZET Amaç:** Derin öğrenme algoritmaları kullanılarak geliştirilen otomatik makine öğrenme algoritmaları, son zamanlarda birçok çalışmanın ilgi odağı olmuştur. Bu çalışmanın amacı, kolorektal kansere ilişkin histopatolojik görüntülere ait doku örneklerinin bilinen 8 farklı histopatolojik doku tiplerine göre sınıflandırmasını yapabilecek, kolorektal kanser tanısında hekimlere klinik destek verebilecek ve bu sayede hekimlerin hızlı ve doğru karar verebilmelerine imkân sağlayabilecek web tabanlı bir yazılım geliştirmektir. **Ge-reç ve Yöntemler:** Bu çalışmada, kolorektal kansere ait farklı histopatolojik doku tiplerini içeren 5.000 histopatolojik görüntüden oluşan açık erişimli veri seti (DOI: 10.5281/zenodo.53169) kullanılmıştır. Geliştirilen yazılımdaki derin öğrenme algoritmasının oluşturulmasında Python programlama dilinde kullanılan Keras/AutoKeras kütüphanesi, kolorektal kansere ait histopatolojik doku tiplerini sınıflandırmak için uygulanmıştır. Web tabanlı yazılımın geliştirilmesinde Python dili kütüphaneleri kullanıldı. Kolorektal kanserin 8 histopatolojik doku tipini tahmin etmek için derin öğrenmeye dayalı bir model oluşturuldu. **Bulgular:** Farklı doku tipleri için hesaplanan performans ölçütleri arasında en yüksek metrik değerleri adipose için hesaplanmış olup sırasıyla; doğruluk 0.996, duyarlılık 0.992, özgülük 0.996, kesinlik 0.974, geri çekme 0.992 ve F<sub>1</sub>-skoru 0,983 olarak bulunmuştur. Bu araştırma, açık erişim yazılımı içermesi ile diğer çalışmalardan farklıdır. **Sonuç:** Elde edilen deneysel bulgular, geliştirilen bu yazılımın kolorektal kansere ait 8 doku türünün tespiti ve teşhisinde kullanılabilmesini göstermektedir. Geliştirilen yazılım sayesinde kolorektal kansere ait doku türlerinin tıp uzmanları ve diğer sağlık çalışanları tarafından kolayca anlaşılması sağlanmaktadır. Bu sayede tıp uzmanları ve diğer sağlık çalışanlarının iş yükü azalmış olur ve hızlı bir danışma sistemi oluşturulmuş olur.

**Anahtar kelimeler:** Çoklu sınıflandırma; doku tipleri; kolorektal kanser; derin öğrenme mimarisi; Keras/AutoKeras

**Correspondence:** Zeynep KÜÇÜKAKÇALI

Department of Biostatistics and Medical Informatics, İnönü University Faculty of Medicine, Malatya, TURKEY/TÜRKİYE

**E-mail:** zeynep.tunc@inonu.edu.tr



Peer review under responsibility of Türkiye Klinikleri Journal of Biostatistics.

**Received:** 17 Feb 2021 **Received in revised form:** 10 Mar 2021 **Accepted:** 10 Mar 2021 **Available online:** 19 Aug 2021

2146-8877 / Copyright © 2021 by Türkiye Klinikleri. This is an open access article under the CC BY-NC-ND license (<http://creativecommons.org/licenses/by-nc-nd/4.0/>).

Cancer is a heterogeneous group of diseases, also defined as a malignant neoplasm, characterized by a clonal increase of abnormal cells. In other words, cancer is defined as the increase in the number and proliferation of abnormal cells that grow excessively into the junction points and other organs of the body, which is also characterized as “metastasis”.<sup>1</sup>

Cancers usually originate from epithelial cells covering surfaces of the body. Colorectal cancers (CRC) are usually carcinomas in the morphology of adenocarcinoma, originating from epithelial cells in the colorectal mucosa. CRC are important types of cancer-related diseases and deaths. This type of cancer is one of the essential reasons for death around the world.<sup>2</sup> CRC is the third most frequently diagnosed cancer in both males and females over the world, with more than a million new cases reported annually. The highest incidences have been reported in the regions where western diet and lifestyle are common, including North America, Australia, New Zealand, and Europe. Asia and Africa are the regions with the lowest incidence of CRC.<sup>3,4</sup> These cancers are generally seen in older people, and their incidence increases significantly with age. According to the data from the United States, the five-year survival of CRC was 65%, and between 1976 and 2000, there was a 26% reduction in CRC-related mortality. Between 2000 and 2013, CRC death rates were reported to decrease by 34% in the population aged 50 and over and 13% in the population aged below 50. The main reasons for this situation may include detection and resection of precancerous polyps by screening methods, diagnosis of CRC at an earlier phase by screening techniques, reduction of risk factors, and improvements in CRC treatment methods.<sup>5,6</sup>

Histopathology is the examination of changes in organs, tissues, and cells under a microscope, by using various methods. The tissues to be examined are first cut into suitable thicknesses for examination by using a micro cutter called a microtome. For staining the sections, generally, hematoxylin and eosin (blue and red-H&E) staining techniques are used, and structures such as nuclei and cytoplasm are made clear by taking different colors.<sup>7,8</sup> The next procedure is the detection phase, and the disease is diagnosed as a result of the examination. The information obtained by histopathological studies sheds light on the microscopic structure of tissues. It is used to make a diagnosis by using different pathological features of various diseases in the tissues. It is used for accurate and precise diagnosis of many diseases, especially cancer.

Early diagnosis is very important for the prevention and reduction of the deaths caused by cancer. The accurate medical interventions in the early period increase the chance of survival. Biopsy has been used as the gold standard method in the diagnosis of cancer. In the biopsy procedure, samples taken from tissues thought to be risky are examined by specialist pathologists under appropriate microscopes. Training and specialization of pathologists for the examination of the collected tissue pieces and the decision-making phase is a very long and costly process. Even if these processes have been successfully completed, different pathologists can make different decisions for the same piece of tissue. In order to eliminate these differences, image processing methods that can calculate using quantitative data are used.<sup>9</sup>

Deep learning (DL) is an artificial intelligence technique that utilizes multi-layered artificial neural network (ANN) modeling in the fields such as object recognition, speech recognition, and natural language data processing.<sup>10</sup> DL techniques used in the domain of medical image processing have shown an impressive performance during recent years. Unlike traditional machine learning (ML) methods, DL can automatically learn from the icons of data of images, videos, sounds, and texts instead of learning by coded rules. It can also learn from a raw image or text data, and thanks to its flexible structure, the accuracy can be enhanced depending on the magnitude of the relevant data.<sup>11</sup>

The objective of the current paper is to design a web-based software that can classify tissue samples of CRC according to eight different histopathological tissue types, to support physicians for the clinical diagnosis of CRC, and thus to enable physicians to make quick and accurate decisions.

## MATERIAL AND METHODS

### DATASET

In this study, an open-access dataset (<http://doi.org/10.5281/zenodo.53169>) consisting of 5,000 histopathological images containing eight tissue types of CRC was used. All raw data on CRC tissue types were published under the title of “Creative Commons Attribution 4.0 International License (<http://creativecommons.org/licenses/by/4.0/>)”. All the details of the processes regarding the obtaining of the examined types of CRC, including low-level and high-level tumors, and rescaling the images of the tissues were given in that study.<sup>12</sup>

These eight different tissue types are tumor, stroma (includes homogeneous composition tumor stroma, extra-tumoral stroma, and smooth muscle), complex (includes single tumor cells and/or several immune cells), lympho (contains immune cell conglomerates and sub-mucosal lenfoid follicles), debris (contains necrosis, bleeding and mucus), mucosa (normal mucosal glands), adipose, and empty (no tissue). Representative images taken from the related dataset regarding the histopathological images are given in [Figure 1](#). The first ten images of each type of tissue are seen in the dataset. In routine histopathological images, they reflect the large variety of illumination, stain intensity, and tissue textures present. The images from ten different samples of primary colorectal tumors were collected in this study. In order to avoid any bias concerning the average grayscale intensity, it was provided that each of the examined tissue types contains both bright and dark samples.<sup>12</sup>

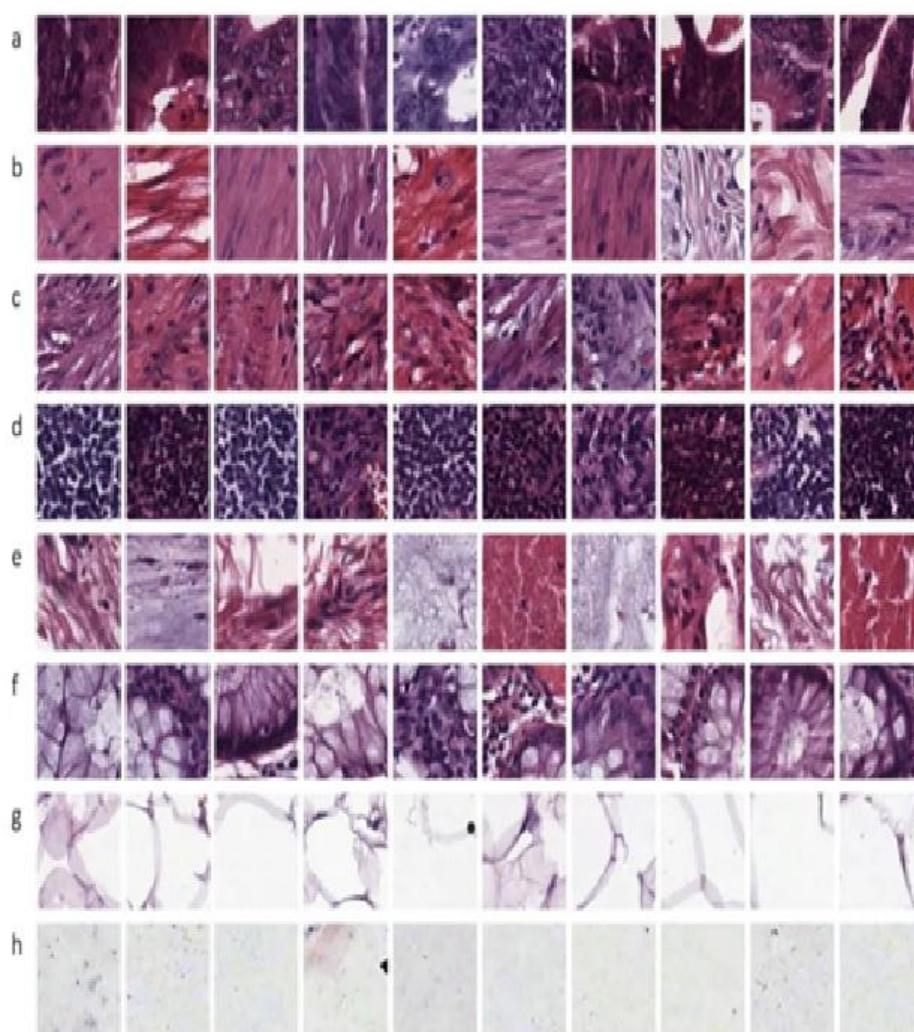


**FIGURE 1:** Histopathological view of eight different tissue types (a: Tumor; b: Stroma; c: Complex; d: Lympho; e: Debris; f: Mucosa; g: Adipose, h: Empty).<sup>12</sup>

Samples within an image data set defined for a specific purpose are a region of interest. The concept of region of interest is widely employed in many fields; especially, in medical imaging, the borders of a tumor can be specified on an image or in volume to measure its size.<sup>13</sup> In the current study, [Figure 2](#) illustrates the tissue types of the identified regions of interest from a series of separate, larger 5000x5000pxH&E images of CRC.

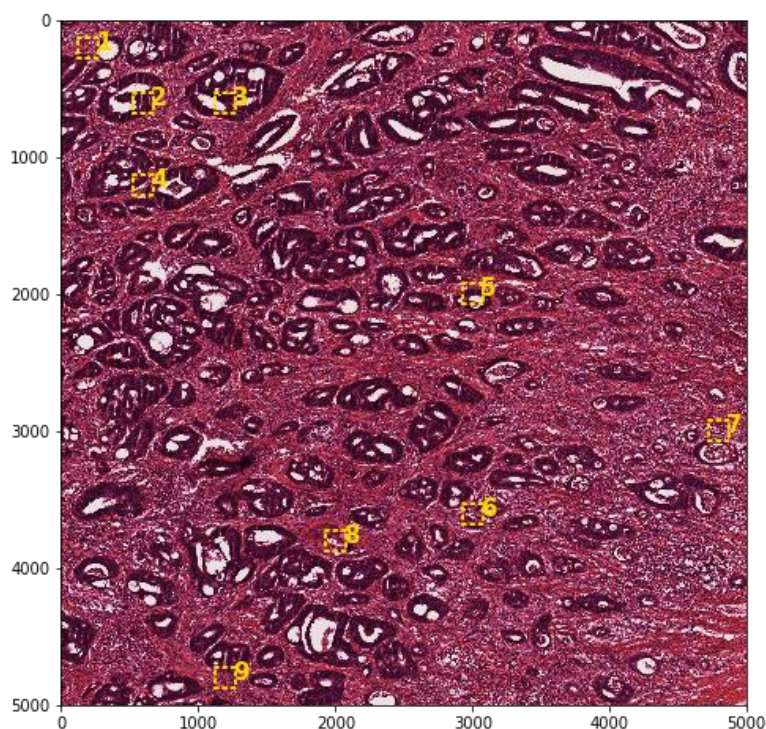


**FIGURE 2:** The tissue types of the identified regions of interest.

## DEEP LEARNING APPROACH

DL is a subclass of the ML approach and uses several non-linear processing unit layers for extracting and converting the attributes/features. Each consecutive layer receives the output from the prior layer as input.<sup>14</sup> In DL architecture, there exists a structure based on the learning of several attribute/feature levels or data representations. Top-level features are extracted from low-level features and establish a hierarchic representation. This representation learns many levels of representation, which correspond to several grades of abstraction. DL is based on learning from the data representation as to the basic structure. For example, representation of an image may include properties such as a vector of density values per pixel, edge sets, and special shapes. Some of the features/attributes exemplify the data better. At this phase, the advantage of DL is that it uses effective algorithms to obtain a hierarchical feature that best represents the data, instead of hand-crafted features.<sup>15</sup>

ANNs are structures developed by inspiring the neuronal structure of the human brain. The ANN collects the information coming to the nerve cells and produces the output by passing it through the specified activation function. Multi-layer ANNs, on the other hand, consist of the input layer in which the inputs are represented, the hidden layers, where the information obtained from the input layer is converted to an output, and the output layer, where the results from the last hidden layer are converted to output values.<sup>16,17</sup> Convolutional neural network (CNN) is a DL method that is frequently used in computerized image recognition

studies and gives very successful results. In CNN, unlike multi-layered ANN, the convolution process (circulation of filters on input for feature extraction) is used in at least one of its layers, instead of using matrix multiplication. Feature extraction is implemented by using filters on the input given in the first layers. At the same time, the size reduction functions are used both for reducing the cost of calculation and transferring the summarized information of the features learned from the input to the other layers. Then, these properties obtained from the input are transformed into a one-dimensional vector, and the classification process is performed by giving them as inputs to the fully connected layer or layers.<sup>18</sup>

AutoKeras is an automated ML technique included in the Keras library in Python programming. AutoKeras ensures appropriate functions to seek for the architecture and hyperparameters of DL approaches automatically. The purpose of the system in question is to automatically create DL structures to predict any target features, such as a disease.<sup>19</sup> A detailed description of the AutoKeras system is shown in [Figure 3](#).

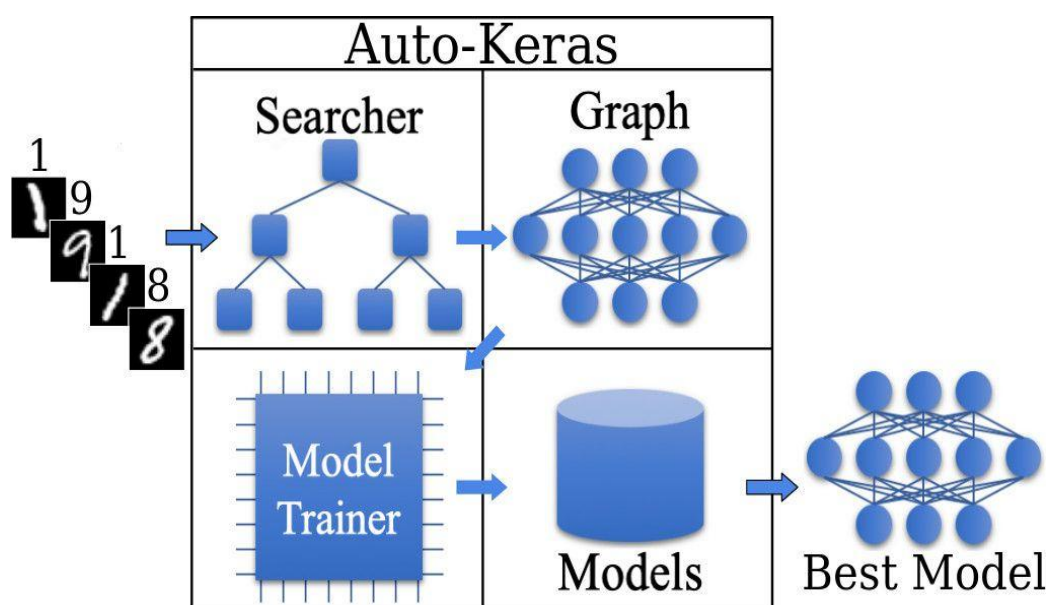


FIGURE 3: A detailed description of the AutoKeras system.<sup>19</sup>

In this study, histopathological images of eight different tissue types related to CRC were used for classification. In this study, a total of 5,000 histopathological images were used for analysis. As a hold-out strategy, 4,000 (80%) of them were allocated as a training dataset, and the remaining 1,000 (20%) images were selected as a testing dataset, randomly. In the random selection for the images of the training dataset, “random.choice()” function in Python was employed throughout the stages. In the image preprocessing (image rotation, altering width and length, pruning images, rescaling, etc.) stage, Keras/AutoKeras library from the Python programming language was employed for the preprocessing of images in which raw image data is processed to minimize visual uncertainty and noise as well as make it more usable for subsequent steps.<sup>19,20</sup> Common tasks in this stage encompass normalization of the pixel intensity to deal with artifacts of luminance and image scaling to lessen the representation size. During the training stage, more data augmentation was conducted in the form of tile rotations and color changes to improve robustness and accumulate regularization to the system.<sup>21</sup>

The Bayesian optimization algorithm was used to determine the best neural network architecture and hyperparameters in the AutoKeras system created in this study. Detailed information on the proposed AutoKeras system is given in [Table 1](#).

**TABLE 1:** Detailed information about the proposed AutoKeras architecture.

Layer number	Layer (type)	Output Shape	Param #	Connected to	Config
1	Input_1 (Inputlayer)	(None, 64, 64, 3)	0		
2	Activation_1 (Activation)	(None, 64, 64, 3)	0	input_1[0][0]	activation: relu
3	Activation_10 (Activation)	(None, 64, 64, 3)	0	activation_1[0][0]	activation: relu
4	Activation_8 (Activation)	(None, 64, 64, 3)	0	activation_1[0][0]	activation: relu
5	Conv2d_9 (Conv2D)	(None, 64, 64, 3)	12	activation_10[0][0]	activation: linear, filters: 3, kernel_size: (1,1), strides: (1,1)
6	Add_3 (Add)	(None, 64, 64, 3)	0	activation_8[0][0] conv2d_9[0][0]	
7	Conv2d_8 (Conv2D)	(None, 64, 64, 6)	168	add_3[0][0]	activation: linear, filters: 6, kernel_size: (3,3), strides: (1,1)
8	Batch_Normalization_1 (Batchnor)	(None, 64, 64, 3)	12	activation_1[0][0]	Momentum: 0.99, epsilon: 0.001
9	Activation_9 (Activation)	(None, 64, 64, 6)	0	conv2d_8[0][0]	activation: relu
10	Conv2d_1 (Conv2D)	(None, 64, 64, 64)	1792	batch_normalization_1[0][0]	activation: linear, filters: 64, kernel_size: (3,3), strides: (1,1)
11	Conv2d_6 (Conv2D)	(None, 64, 64, 64)	448	activation_9[0][0]	activation: linear, filters: 64, kernel_size: (1,1), strides: (1,1)
12	Add_2 (Add)	(None, 64, 64, 64)	0	conv2d_1[0][0] conv2d_6[0][0]	
13	Max_Pooling2d_1 (Maxpooling2d)	(None, 32, 32, 64)	0	add_2[0][0]	pool_size: (2,2), strides: (2,2)
14	Activation_2 (Activation)	(None, 32, 32, 64)	0	max_pooling2d_1[0][0]	activation: relu
15	Batch_Normalization_4 (Batchnor)	(None, 32, 32, 64)	256	activation_2[0][0]	momentum: 0.99, epsilon: 0.001
16	Batch_Normalization_2 (Batchnor)	(None, 32, 32, 64)	256	batch_normalization_4[0][0]	momentum: 0.99, epsilon: 0.001
17	Activation_6 (Activation)	(None, 32, 32, 64)	0	batch_normalization_2[0][0]	activation: relu
18	Conv2d_2 (Conv2D)	(None, 32, 32, 512)	295424	activation_6[0][0]	activation: linear, filters: 512, kernel_size: (3,3), strides: (1,1)
19	Max_Pooling2d_2 (Maxpooling2d)	(None, 16, 16, 512)	0	conv2d_2[0][0]	pool_size: (2,2), strides: (2,2)
20	Activation_3 (Activation)	(None, 16, 16, 512)	0	max_pooling2d_2[0][0]	activation: relu
21	Batch_Normalization_3 (Batchnor)	(None, 16, 16, 512)	2048	activation_3[0][0]	momentum: 0.99, epsilon: 0.001
22	Max_Pooling2d_6 (Maxpooling2d)	(None, 16, 16, 64)	0	batch_normalization_2[0][0]	pool_size: (2,2), strides: (2,2)
23	Conv2d_7 (Conv2D)	(None, 16, 16, 512)	262656	batch_normalization_3[0][0]	activation: linear, filters: 512, kernel_size: (1,1), strides: (1,1)
24	Activation_7 (Activation)	(None, 16, 16, 64)	0	max_pooling2d_6[0][0]	activation: relu
25	Max_Pooling2d_4 (Maxpooling2d)	(None, 32, 32, 3)	0	batch_normalization_1[0][0]	pool_size: (2,2), strides: (2,2)
26	Conv2d_3 (Conv2D)	(None, 16, 16, 128)	589952	conv2d_7[0][0]	activation: linear, filters: 128, kernel_size: (3,3), strides: (1,1)
27	Conv2d_5 (Conv2D)	(None, 16, 16, 128)	8320	activation_7[0][0]	activation: linear, filters: 128, kernel_size: (1,1), strides: (1,1)
28	Max_Pooling2d_5 (Maxpooling2d)	(None, 16, 16, 3)	0	max_pooling2d_4[0][0]	pool_size: (2,2), strides: (2,2)
29	Add_1 (Add)	(None, 16, 16, 128)	0	conv2d_3[0][0] conv2d_5[0][0]	
30	Activation_5 (Activation)	(None, 16, 16, 3)	0	max_pooling2d_5[0][0]	activation: relu
31	Concatenate_1	(None, 16, 16, 131)	0	add_1[0][0] activation_5[0][0]	
32	Conv2d_4 (Conv2D)	(None, 16, 16, 64)	8448	concatenate_1[0][0]	activation: linear, filters: 64, kernel_size: (1,1), strides: (1,1)
33	Max_Pooling2d_3 (Maxpooling2d)	(None, 8, 8, 64)	0	conv2d_4[0][0]	pool_size: (2,2), strides: (2,2)
34	Global_Average_Pooling2d_1 (Glo)	(None, 64)	0	max_pooling2d_3[0][0]	
35	Dropout_1 (Dropout)	(None, 64)	0	global_average_pooling2d_1[0][0]	rate: 0.25
36	Dense_1 (Dense)	(None, 64)	4160	dropout_1[0][0]	activation: linear, units: 64
37	Activation_4 (Activation)	(None, 64)	0	dense_1[0][0]	activation: relu
38	Dense_2 (Dense)	(None, 8)	520	activation_4[0][0]	activation: linear, units: 8

## DEVELOPED WEB-BASED SOFTWARE

The developed web-based interface is designed to classify different tissue types from histopathological images of CRC. During the development phase; Libra programming language Keras, TensorFlow, Scikit-learn, OpenCV, Pandas, NumPy, Matplotlib, and Flask libraries were used. The screen image of the designed web-based interface is shown in [Figure 4](#).<sup>19,22-28</sup>

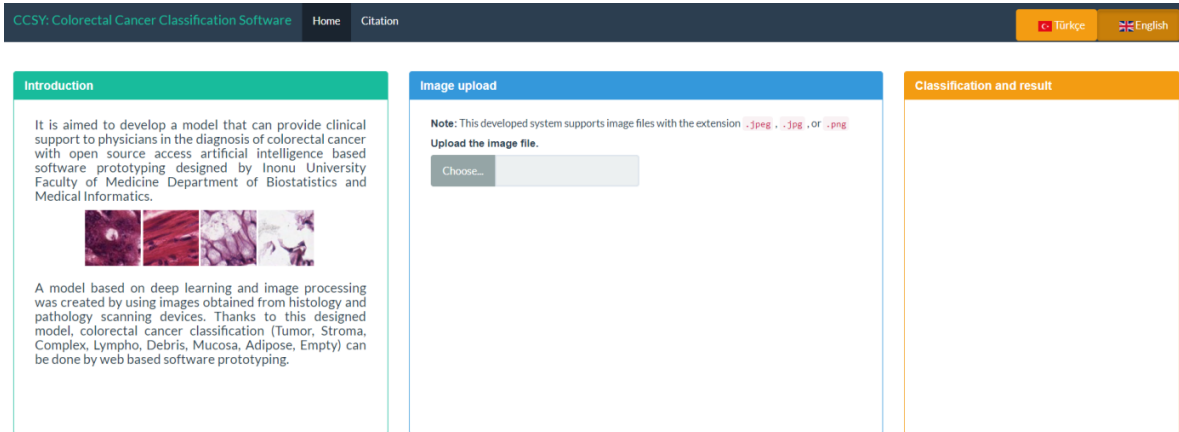


FIGURE 4: Screenshot of the developed web-based software.

The developed web-based software consists of two menus: “Home” and “Citation”. “Home” the main menu consists of three sub-menus, including “Introduction”, “Image Upload”, and “Classification and Result”. Brief information about the software is included in the “Introduction” sub-menu. The image to be analyzed is transferred to the web-based software by the “Image Upload” sub-menu. The developed software can work with image files with the extensions of .jpeg, .jpg, and .png. If the files with different extensions than the files that are supported by the software are loaded, a warning screen will be displayed as “Image Not Suitable” in the “Classification and Result” sub-menu. The screenshot of this warning is given in [Figure 5](#).

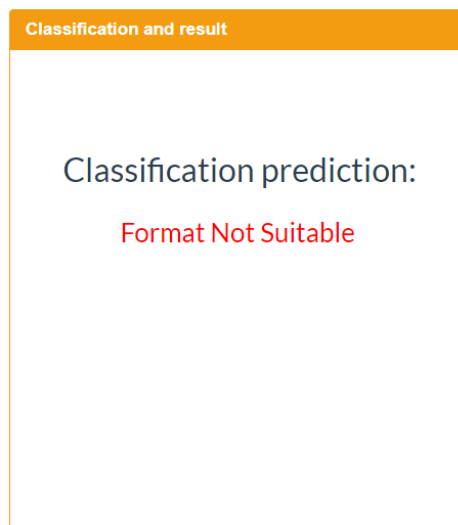


FIGURE 5: File upload error screen with different file extensions.

A min-max filter was created in order that the software can determine the files with different extensions than the files with supported extensions. The  $m \times n$  pixel matrix is estimated for each image in the related filter. Then, the components of the calculated matrix are summed up by the formula given below.

$$A_F = \sum_{i=1}^m \sum_{j=1}^n a_{ij}$$

A min/max value range is determined among the  $A_F$  values obtained in this way. If the  $A_F$  value of the loaded image is beyond the issued range; this image is determined as not suitable. For this process, the pseudo-code is as follows.

**Pseudo-Code I.** Min-max filtering.

**A, B and C are matrices of each RGB channel of uploaded images.**

```

1:  if (A, B and C are not all equal){
2:    return ("Irrelevant image")
3:  } else {
4:    if (AF not in range [2.966.387, 16.439.603]) {
5:      return ("Irrelevant image")
6:    }
7:    else {
8:      return ("Relevant image")
9:    }
10: }

```

Which of the eight classes the uploaded image belongs to is determined in the “Classification and Result” sub-menu output. The software can be reached publicly at <http://biostatapps.inonu.edu.tr/KKSY/>. The software has English and the Turkish language supports.

## PERFORMANCE EVALUATION METRICS

Accuracy, sensitivity, specificity, precision, recall,  $F_1$ -score metrics were employed to evaluate the prediction performance of the constructed model(s) by using the DL algorithm. In the calculation of performance metrics, the developed software DTROC: Diagnostic Tests and ROC Analysis Software was used.<sup>29</sup> The formulas of these metrics are shown below.

$$Accuracy = \frac{TP + TN}{TP + TN + FP + FN}$$

$$Sensitivity = \frac{TP}{FN + TP}$$

$$Specificity = \frac{TN}{FP + TN}$$

$$Precision = \frac{TP}{TP + FP}$$

$$Recall = \frac{TP}{TP + FN}$$

$$F_1 - score = \frac{2 \times TP}{(2 \times TP) + FP + FN}$$

TP: True positive number; TN: True negative number; FP: False positive number; FN: False negative number.



## EXPERIMENTAL RESULTS

Performance metric values for multi-classification of each tissue type of CRC by using the proposed web-based interface are presented in [Table 2](#).

**TABLE 2:** Performance metric values for multi-classification of different tissue types.

Tissue-types \ Metrics	Tumor	Stroma	Complex	Lympho	Debris	Mucosa	Adipose	Empty
Accuracy	0.977	0.986	0.970	0.980	0.994	0.991	0.996	0.996
Sensitivity	0.964	0.917	0.860	0.920	0.980	0.957	0.992	0.975
Specificity	0.979	0.996	0.986	0.988	0.996	0.995	0.996	0.999
Precision	0.850	0.972	0.904	0.916	0.974	0.968	0.974	0.996
Recall	0.964	0.917	0.860	0.920	0.980	0.957	0.992	0.975
F1-score	0.903	0.944	0.881	0.918	0.977	0.962	0.983	0.985

When the calculated performance metrics are examined, the values obtained from the DL model created for the classification of each tissue type were higher than 0.85.

In order to demonstrate the principle of operation of the interface, when a histopathological image belonging to the tumor tissue type is loaded into the web-based software, the output of the prediction of classification is given in [Figure 6](#).

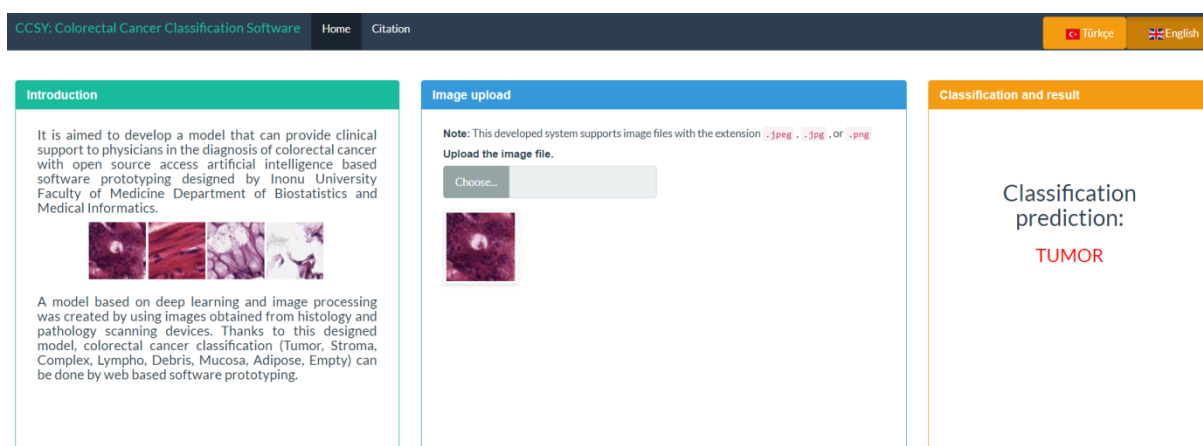


**FIGURE 6:** The output of classification prediction of a histopathological image belonging to the tumor tissue type.

## DISCUSSION

Expert pathologists examine samples taken from risky tissues by histopathology under appropriate microscopes. Training and specialization of pathologists and doctors for the examination of the tissue types taken and the clinical decision-making phase is a very long and costly process. For these reasons, these problems have been tried to be avoided by using image processing methods that can calculate by using quantitative data.<sup>30</sup>

Early studies consisted of a system based on obtaining mathematically determined properties from images. Although these feature extraction techniques determined by the researchers required much experience and they could not achieve high success for every image. Especially, the complex color information in the images makes this process difficult, and a limited level of success is achieved in image processing studies with such features that cannot be determined automatically. In recent years, the developments in artificial intelligence algorithms and computer hardware led to great progress for automatic feature extraction and eliminated the negative effects arising from manually extracted features.<sup>31</sup> CNNs, a DL architecture, are particularly successful for image processing problems and have been widely used in all scientific studies. CNNs automatically extract features from images and can classify these features through their own fully connected networks. Since early diagnosis is very important in the treatment of cancer, it is very important to make a correct and successful determination, while the other important point is to make this analysis in a short time. Recently, image processing and artificial intelligence techniques have been frequently used to shorten the analysis period and to create an additional consultation system for specialists.<sup>32</sup>

The current study develops web-based software that can assort eight different tissue types of CRC, including tumor, stroma, debris, lympho, mucosa, adipose, empty, and complex, based on histopathological images, by using the CNN from DL architectures. It is predicted that clinicians can classify tissues faster and more accurately from histopathological images of CRC by using the developed open-access web-based software. Therefore, the proposed software provides a useful support system in the clinical decision regarding the classification of CRC tissues.

In one study, a DL technique based on CNN was proposed to differentiate adenocarcinomas from healthy tissues and benign lesions for CRC classification, and this CNN model achieved a fairly good classification performance (accuracy rate at the test stage was approximately 90%). Besides, it was reported in that study that transfer learning approaches based on pre-trained CNN models on a completely different dataset (i.e., ImageNet), transfer learning showed better performance (an accuracy rate of 96%) than the DL technique based on the CNN, in the same test dataset. In another study, an effective CNN-based prediction model was designed to label colon cancer images, and the performance of the recommended RCCNet network was compared with popular alternative models such as AlexNet, GoogLeNet, CIFAR-VGG, and Wide Residual Networks (WRNs). The related experimental results of the study revealed that the designed model produced better predictions than the five CCN methods concerning accuracy rate,  $F_1$ -score, and training length.<sup>33</sup> In another study using the same image data set with this study, a classification was made for two tissue types (tumor and stroma) from histopathological images of CRC, and an accuracy rate of 98.6% was obtained. Also, when eight different tissue types of CRC were classified from histopathological images, the accuracy rate was found to be 87.4%.<sup>12</sup> In the multi-class analysis made by using the software developed in this study, 94.4% accuracy of the concerned classification was obtained for eight tissue types from the histopathological images of CRC, which was higher than the accuracy rate (87.4%) obtained from the same image data set, in that study. In another study that examined the same histopathological image data set, when four different methods classified the seven types of colon tissues, the highest accuracy of 100% was obtained only for Adipose, while the highest accuracy value calculated for all classes was 68.7%.<sup>34</sup> With the model proposed in this study, the minimum value of performance criteria calculated for each of the

eight tissue types of CRC was 85%. Given the performance metrics calculated in this study, it was determined that the recommended DL model was able to successfully classify eight tissue types from histopathological images related to CRC. In addition, the most important difference of this research from other studies is the development of an open access web-based software for the classification of multiple tissue types of CRC.

This study may have a few limitations and suggestions for further research. First, higher prediction rates can be obtained by using a larger number of images. Second, the software's prediction performance can be further increased by applying different ML algorithms. Third, the software developed as a prototype may better be tested with images from other cancer types to prove the accuracy and functionality of the software. Fourth, the use of meta-learning and ensemble learning techniques in classifying cancer-type images can result in more clinically useful results. Additionally, many studies have been performed on different health problems and diseases (skin cancer, lung cancer, brain cancer, pneumonia, gastrointestinal cancer, etc.) using Keras DL framework during the last years. This research differs from other studies in that it includes open access software.

## CONCLUSION

In conclusion, the web software based on the model proposed in this study provided promising predictions in classifying different tissue types from histopathological images of CRC. Thanks to the proposed software, the tissue types of CRC are easily understood by medical professionals and other healthcare workers. Hence, the workload of medical professionals can be reduced, and a faster consultation system can be formed. The proposed software supplies a useful support system in the clinical decision regarding the classification of CRC tissues.

### **Source of Finance**

*During this study, no financial or spiritual support was received neither from any pharmaceutical company that has a direct connection with the research subject, nor from a company that provides or produces medical instruments and materials which may negatively affect the evaluation process of this study.*

### **Conflict of Interest**

*No conflicts of interest between the authors and/or family members of the scientific and medical committee members or members of the potential conflicts of interest, counseling, expertise, working conditions, share holding and similar situations in any firm.*

### **Authorship Contributions**

**Idea/Concept:** Emek Güldoğan, Hasan Ucuzal, Cemil Çolak; **Design:** Emek Güldoğan, Hasan Ucuzal; **Control/Supervision:** Zeynep Küçükakçalı, Emek Güldoğan; **Data Collection and/or Processing:** Hasan Ucuzal; **Analysis and/or Interpretation:** Hasan Ucuzal, Emek Güldoğan, Zeynep Küçükakçalı; **Literature Review:** Zeynep Küçükakçalı, Cemil Çolak; **Writing the Article:** Zeynep Küçükakçalı; **Critical Review:** Cemil Çolak; **References and Fundings:** Cemil Çolak; **Materials:** Hasan Ucuzal, Cemil Çolak.

## REFERENCES

1. Yardım N, Mollahaliloğlu S, Bora Başara B. Türkiye'de kanser durumu ve uluslararası göstergeler ile uyumun değerlendirilmesi. Tuncer AM, Özgül N, Olcayto E, Gültekin, editörler. Türkiye'de Kanser Kontrolü. Ankara: Koza Matbaacılık; 2009. p.51-63. [\[Link\]](#)
2. Ferlay J, Shin HR, Bray F, Forman D, Mathers C, Parkin DM. Estimates of worldwide burden of cancer in 2008: GLOBOCAN 2008. *Int J Cancer*. 2010;127(12):2893-917. [\[Crossref\]](#) [\[PubMed\]](#)
3. Siegel RL, Sahar L, Robbins A, Jemal A. Where can colorectal cancer screening interventions have the most impact? *Cancer Epidemiol Biomarkers Prev*. 2015;24(8):1151-6. [\[Crossref\]](#) [\[PubMed\]](#)
4. Parkin DM, Bray F, Ferlay J, Pisani P. Global cancer statistics, 2002. *CA Cancer J Clin*. 2005;55(2):74-108. [\[Crossref\]](#) [\[PubMed\]](#)
5. Siegel RL, Miller KD, Jemal A. Cancer statistics, 2016. *CA Cancer J Clin*. 2016;66(1):7-30. [\[Crossref\]](#) [\[PubMed\]](#)
6. Ciombor KK, Wu C, Goldberg RM. Recent therapeutic advances in the treatment of colorectal cancer. *Annual Review of Medicine*. 2015;66:83-95. [\[Crossref\]](#)
7. Basavanthally A, Yu E, Xu J, Ganesan S, Feldman M, Tomaszewski J, et al. Incorporating domain knowledge for tubule detection in breast histopathology using O'Callaghan neighborhoods. *Medical Imaging. 2011: Computer-Aided Diagnosis*. 2011. [\[Crossref\]](#)
8. Paramanandam M, O'Byrne M, Ghosh B, Mammen JJ, Manipadam MT, Thamburaj R, et al. Automated segmentation of nuclei in breast cancer histopathology images. *PLoS One*. 2016;11(9):e0162053. [\[Crossref\]](#) [\[PubMed\]](#) [\[PMC\]](#)
9. Bayramoglu N, Kannala J, Heikkilä J. Deep learning for magnification independent breast cancer histopathology image classification. 23rd International conference on pattern recognition. 2016; December 4-8; Cancun, Mexico. [\[Crossref\]](#)
10. Talo M, Baloglu UB, Yıldırım Ö, Acharya UR. Application of deep transfer learning for automated brain abnormality classification using MR images. *Cognitive Systems Research*. 2019;54:176-88. [\[Crossref\]](#)
11. Kaya U, Yılmaz A, Dikmen Y. [Deep Learning Methods used in the field of Health]. *Avrupa Bilim ve Teknoloji Dergisi*. 2019(16):792-808. [\[Link\]](#)
12. Kather JN, Weis C-A, Bianconi F, Melchers SM, Schad LR, Gaiser T, et al. Multi-class texture analysis in colorectal cancer histology. *Scientific Reports*. 2016;6(1):27988. [\[Crossref\]](#)
13. Xu J, Luo X, Wang G, Gilmore H, Madabhushi A. A Deep Convolutional Neural Network for segmenting and classifying epithelial and stromal regions in histopathological images. *Neurocomputing*. 2016;191:214-23. [\[Crossref\]](#) [\[PubMed\]](#) [\[PMC\]](#)
14. Deng L, Yu D. Deep learning: methods and applications. *Foundations and Trends® in Signal Processing*. 2014;7(3-4):197-387. [\[Crossref\]](#)
15. Bengio Y. Learning deep architectures for AI. *Foundations and Trends® in Machine Learning*. 2009;2(1):1-127. [\[Crossref\]](#)
16. Sincen M, Burak K, Yıldız Ö. [Artificial neural network based early warning system for aydin province towards air factors which primarily affect human health]. *Gazi Üniversitesi Fen Bilimleri Dergisi Part C: Tasarım ve Teknoloji*. 2017;5(4):121-31. [\[Link\]](#)
17. Ucuzal H, Yaşar Ş, Çolak C. Classification of brain tumor types by deep learning with convolutional neural network on magnetic resonance images using a developed web-based interface. 3rd International Symposium on Multidisciplinary Studies and Innovative Technologies. 2019 Oct 11-13; Ankara, Turkey: IEEE; 2019. [\[Crossref\]](#)
18. Goodfellow I, Bengio Y, Courville A. Deep learning. ABD: MIT press; 2016. [\[Link\]](#)
19. Jin H, Song Q, Hu X. Auto-keras: An efficient neural architecture search system. Paper presented at: Proceedings of the 25th ACM SIGKDD International Conference on Knowledge Discovery & Data Mining. 2002 Aug 3-7; NY, United States: Association for Computing Machinery; 2019. [\[Crossref\]](#)
20. Gulli A, Pal S. Deep Learning with Keras. Birmingham: Packt Publishing Ltd; 2017. [\[Link\]](#)
21. Arevalo J, Cruz-Roa A, González FA. Histopathology image representation for automatic analysis: A state-of-the-art review. *Revista Med*. 2014;22(2):79-91. [\[Link\]](#)
22. Abadi M, Barham P, Chen J, Chen Z, Davis A, Dean J, et al. Tensorflow: A system for large-scale machine learning. Paper presented at: 12th USENIX Symposium on Operating Systems Design and Implementation OSDI '16'. 2016. [\[Link\]](#)
23. Pedregosa F, Varoquaux G, Gramfort A, Michel V, Thirion B. Scikit-learn: Machine learning in Python. *Journal of Machine Learning Research*. 2011;12:2825-30. [\[Link\]](#)
24. Bradski G, Kaehler A. Learning OpenCV. 1st ed. ABD: O'Reilly Media. Inc; 2008. [\[Link\]](#)
25. McKinney W. pandas: a foundational Python library for data analysis and statistics. *Python for High Performance and Scientific Computing*. 2011;14(9):1-9. [\[Link\]](#)
26. Walt Svd, Colbert SC, Varoquaux G. The NumPy array: a structure for efficient numerical computation. *Computing in Science & Engineering*. 2011;13(2):22-30. [\[Crossref\]](#)
27. Tosi S. Matplotlib for Python Developers. ABD: Packt Publishing Ltd; 2009. [\[Link\]](#)
28. Grinberg M. Flask Web Development: Developing Web Applications With Python. 2nd ed. California: O'Reilly Media, Inc; 2018. [\[Link\]](#)
29. Yasar S, Arslan AK, Yologlu S, Colak C. DTROC: Tanı Testleri ve ROC Analizi Yazılımı [Web-tabanlı yazılım]. 2019. [\[Link\]](#)
30. Hamilton PW, Bankhead P, Wang Y, Hutchinson R, Kieran D, McArt DG, et al. Digital pathology and image analysis in tissue biomarker research. *Methods*. 2014;70(1):59-73. [\[Crossref\]](#) [\[PubMed\]](#)
31. LeCun Y, Bengio Y, Hinton G. Deep learning. *Nature*. 2015;521(7553):436-44. [\[Crossref\]](#) [\[PubMed\]](#)

32. Sirinukunwattana K, Ahmed Raza SE, Yee-Wah Tsang, Snead DR, Cree IA, Rajpoot NM. Locality sensitive deep learning for detection and classification of nuclei in routine colon cancer histology images. *IEEE Trans Med Imaging*. 2016;35(5):1196-206. [[Crossref](#)] [[PubMed](#)]
33. Basha SS, Ghosh S, Babu KK, Dubey SR, Pulabaigari V, Mukherjee S. Rccnet: An efficient convolutional neural network for histological routine colon cancer nuclei classification. 15th International Conference on Control, Automation, Robotics and Vision. 2018 Nov 18-21; Singapore; 2018. [[Link](#)]
34. Ly T, Sarkar R, Skadron K, Acton ST. Classifying images in a histopathological dataset using the cumulative distribution transform on an automata architecture. 2017 IEEE Global Conference on Signal and Information Processing. 2017 Nov 14-16; Montreal, Canada; 2017. [[Crossref](#)]